On the polytropic coefficient of negative ions for modeling the sheath and presheath of electronegative plasmas

L. Schiesko, St. Lishev, A. Revel, E. Carbone, T. Minea

On the polytropic coefficient of negative ions for modelling the sheath and presheath of electronegative plasmas

L. Schiesko,[1, 2, a)] St. Lishev,[3] A. Revel,[2] E. Carbone,[4, b)] and T. Minea[2]
[1)] *IRFM, CEA Cadarache, 13108 Saint-Paul-lez-Durance, France*
[2)] *Université Paris-Saclay, CNRS, Laboratoire de physique des gaz et des plasmas, 91405, Orsay, France*
[3)] *Faculty of Physics, Sofia University, BG-1164 Sofia, Bulgaria*
[4)] *Institut National de la Recherche Scientifique, centre Énergie Matériaux Télécommunications, 1650 blvd Lionel Boulet, J3X 1P7 Varennes, QC, Canada*

(Dated: 1 August 2023)

The fluid description is widely used for the multi-dimensional modeling of low temperature plasmas with complex chemistries due to their relative low computational cost. It relies however on a series of simplifying assumptions and some truncation of the moment equations for describing the non-equilibrium between the electrons, positive ions, negative ions and the neutrals. In this paper, the classical assumption of isothermal negative ions is revisited for electronegative plasmas and more particularly for the fluid modelling of the transition between the plasma and its sheath. To do so, and in contrast to previous studies, the energy balance equation for the negative ions is also computed and it allows to derive the polytropic coefficient γ of the negative ions in addition to the one of the positive ions. Strong variations in the sheath and presheath of the negative ions temperature and their polytropic coefficient are observed. The polytropic coefficient is shown to be a strongly varying function of space having for consequence that the negative ions are isothermal only in a very narrow extension of the presheath. For the case considered in this paper, both positive and negative ion flows are nearly adiabatic at the sheath-edge and become adiabatic inside the sheath. This paper shows that classical fluid modelling assumptions need to be verified for each system under consideration, most particularly while modelling the transition from a plasma to a wall.

Keywords: Thermodynamics, Sheath, Presheath, Multi-fluid, Negative ions, Polytropic coefficient

I. INTRODUCTION

Despite being one of the oldest plasma problems[1,2], the interaction between a plasma and a boundary is still an intense area of research due its numerous applications in plasma processes[3–5]. However, intrinsic difficulties arise in the theoretical description of the plasma boundary because the use of some simplifying assumptions is needed to describe the non-equilibrium transition between the plasma and the wall. A kinetic analysis, consisting in finding the solutions of the Boltzmann or Fokker-Planck equations[6–12] or, if collisions are neglected, the Vlasov equation[13–17], is often required to account both for the microscopic boundary conditions and the inhomogeneity due to space charge. It is however difficult with a kinetic model, in comparison with a self-consistent fluid model, to realistically simulate the geometric effects as well as elementary processes together with a detailed description of the electron and ion collisional processes. The use of Particle-in-Cell codes[22–25] is also possible but the computational effort that would be required to achieve a steady-state solution (for example, 5 days when using the code described by Schiesko et al.[25] for a 1D

[a)] Electronic mail: loic.schiesko@cea.fr
[b)] Electronic mail: emile.carbone@inrs.ca

problem), make them unsuitable to perform parametric scans in 2D or 3D and they are often restricted to small simulation domains in the case of high densities (i.e. small Debye length). For these reasons, the fluid approximation is often used to model non-equilibrium low temperature plasmas[26–29].
In the fluid formalism, the macroscopic properties of the plasma are described by a set of moment equations which are derived from an underlying kinetic equation, usually the Boltzmann equation, well suited for describing plasma discharges. The fluid equations are not closed but involve higher orders of the velocity moments. Truncation procedures exist[26–28] at the cost of eliminating or approximating certain features of the plasma dynamics and constrain the regime of validity of the set of fluid equations. Fluid models are based on the continuity equations resolved both in space and time and they allow describing the evolution of the state of system using a set of independent variables which stem from thermodynamics. However, their validity and application range have been extended in some cases far beyond the cases where the assumption of local thermal equilibrium is valid while still using some thermodynamic properties for truncating the moment equations (e.g. isothermal or adiabatic properties for some species in a multi-species system). Moreover, a common assumption is that the electron energy distribution function in the plasma is governed by the local equilibrium between the acceleration given by the electric field and the momentum and energy losses due to the collisions[18]. Computing rate and transport coefficients usually allows to assimilate the temperature to a mean energy which is then used in the energy continuity equation[19–21]. The use of fluid equations can therefore be extended beyond Maxwellian distribution functions using non-equilibrium factors (such as Kappa or Druyvesteyn velocity distribution functions) although their applicability is not often well justified. This is underlined by the difficulty to set proper boundary conditions and the sensitivity of fluid models to initial values to yield physical results while solving the set of equations for the steady state.
Typically, the continuity and momentum exchange equations are used for the positive ions while the electrons and, when included, the negative ions, are assumed to follow a Boltzmann relation[30–33] although Franklin[34] showed in his seminal paper that care should be taken when using Boltzmann relations both for electrons and negative ions. Two-fluid models for electropositive plasmas, where continuity and momentum exchanges equation are used also for the electrons, are less common[35–38].

To test the validity of fluid models and particularly the transition of a plasma to a wall, it is useful to check the thermodynamic characteristics of the fluid and their consistency with the general hypotheses made while constructing the model. The description of the plasma sheath is concerned with the interactions between a closed system and its environment and one can expect the particles to behave either as isothermal, isentropic or adiabatic. Particle and energy balance equations in the fluid approximation (i.e. where the velocity distributions are described with a single parameter such as the temperature or the mean energy) for a closed system do not fulfil *a priori* any particular thermodynamic case although its formalism usually implies the fulfilment of local thermal equilibrium (LTE) for single species. The departure from LTE of a system is, in the most simple case, done by relaxing the condition of a single temperature for all species and allowing different temperatures which are controlled by their predefined velocity distribution at an injection boundary and/or via the coupling with external fields. Their ratio is then driven by the interaction of the system with its environment and the momentum exchanges between the species inside the system. For non-equilibrium plasmas, it is typically a strong electric field that increases the temperature of the electrons (due to their low mass compared to all the other species) within the plasma region and they do not have enough time and space to thermalize with the surrounding species nor the environment.

In the vast majority of studies, the truncation of the fluid equations occurs at the momentum exchange equation, which requires an assumption about the higher moment of the distribution function, the pressure force term ∇p. A common approach is to relate it to the

density gradient by the ansatz

$$\nabla p = \gamma k_B T \nabla n \tag{1}$$

where γ is the polytropic coefficient[39], n the density, k_B the Boltzmann constant and T the temperature. For the description of multi-fluid systems, it is therefore also usual to assume some properties like isentropic, isothermal or adiabatic flows where each species take a single value of γ and the latter describes globally its interaction with the environment.

The polytropic coefficient is defined by $\gamma = (c - c_p)/(c - c_V)$ where c is the polytropic specific heat and c_p and c_V are the specific heat at constant pressure and constant volume respectively. In that case, the system exchanges no energy with the environment. In the case of ideal gas law, the relation $p = nk_BT$ describes the properties of a gas made of non-interacting particles and using the ansatz given by equation 1, one gets

$$\gamma = 1 + \frac{n}{T}\frac{\nabla T}{\nabla n}. \tag{2}$$

This equation, with γ expressed as a function of spatial coordinates, gives the local thermodynamic properties of the fluid flow in the approximation of an ideal gas. A well-known special case is the adiabatic case for which $\delta Q = 0$ corresponding to $c = 0$ and yielding $\gamma = c_p/c_V$[1]. Concerning the positive ions temperature T_i, the assumption mostly used is a constant value. Setting $\gamma = 1$ corresponds to an isothermal ion flow[40–42], while setting $\gamma = 3$ yields to a one-dimensional adiabatic ion flow[43–46]. It has been shown however by Kuhn et al.[39] that γ for positive ions is not a constant and varies spatially for low temperature non-equilibrium plasmas. This finding demonstrates the inconsistency of the isothermal or adiabatic assumption or even any other constant γ value for modelling the ion flow in the sheath and the presheath. A two-fluid model for positive ions and electrons has been recently developed where $\gamma(x)$ and $T_i(x)$ both become functions of a spatial coordinate[47–50]. Concerning the description of the negative ions and the problem of the electronegative plasma sheath, and to the best of the authors' knowledge, the use of a Boltzmann factor with the isothermal assumption is the rule and it is generally adopted[30–34,37,51,52] .

In view of the above, it is legitimate to question the validity of the assumptions of a constant temperature and of a constant γ for the negative ions in the sheath and presheath. In this paper, a multi-fluid model[47–50] is extended to account for the negative ions with γ(x) and $T(x)$ computed self-consistently, neglecting the heat flux for all the involved species. In section II the equations are presented and mathematically converted to an explicit 1^{st} order system with the advantage of directly identifying the singularities and giving the possibility to determine boundary and initial conditions values leading to physically acceptable solutions. In section III the results are presented and discussed. First the validity of the model is demonstrated by considering $T_i = 0$ as initial condition. The polytropic coefficients of the positive and negative ions are then investigated with $T_i \neq 0$ as well as their temperature profiles. Finally, section IV summarizes the main conclusions.

II. THE MODEL

A. Assumptions and description of the model

One considers a one-dimensional model with the plasma bulk located at x = 0, as shown in Figure 1 and it expands towards positive x values without the explicit definition of a wall. Details of the derivation of the fluid equations from the moments of the Boltzmann equation

[1] Note that using the ideal gas law as equation of state for an adiabatic expansion is by definition equivalent of having an isentropic gas flow.

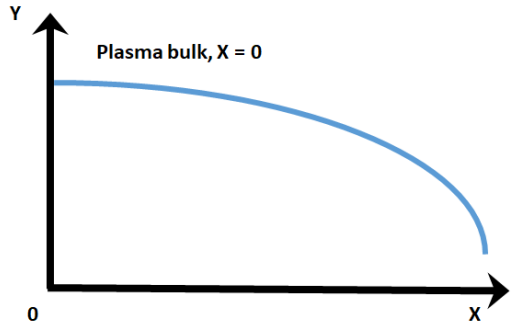

FIG. 1. Schematic representation of the model setup. The plasma bulk is located at x = 0 and expands. The blue line is a representation of an observable such as the electric potential or the density.

can be found in there[47,48]. The steady state fluid equations are written in the following form with $\alpha \in$ [i,e,n] for the positive ions, electrons and negative ions respectively:

$$\frac{\partial}{\partial x}(n_\alpha u_\alpha) - S_\alpha = 0 \tag{3}$$

$$m_\alpha n_\alpha u_\alpha \frac{\partial u_\alpha}{\partial x} + \frac{\partial p_\alpha}{\partial x} \underset{e,n}{\overset{i}{\pm}} e_0 n_\alpha \frac{\partial \phi}{\partial x} - A_\alpha + m_\alpha u_\alpha S_\alpha = 0 \tag{4}$$

and for the positive and negative ions, i.e., $\alpha \in$ [i,n]:

$$\frac{1}{2}u_\alpha \frac{\partial p_\alpha}{\partial x} + \frac{3}{2}p_\alpha \frac{\partial u_\alpha}{\partial x} - M_\alpha + u_\alpha A_\alpha - \frac{1}{2}m_\alpha u_\alpha^2 S_\alpha = 0 \tag{5}$$

The potential profile ϕ is determined by the Poisson Equation:

$$\frac{\partial^2 \phi}{\partial^2 x} = -\frac{e_0}{\epsilon_0}(n_i - n_e - n_n) \tag{6}$$

where n_i, n_e and n_n are the positive ion, electron and negative ion densities respectively, u_i, u_e and u_n are the positive ion, electron and negative ion fluid velocities respectively, e_0, m_α and ϵ_0 the elementary charge, mass and the vacuum permittivity respectively. The source terms S_α, the elastic collisions terms A_α and the energy transfer terms M_α are typically prescribed functions.

The pressure term appearing in eq. (4) is written

$$\frac{\partial p_e}{\partial x} = k_B T_e \frac{\partial n_e}{\partial x} \tag{7}$$

For the positive and negative ions, the closure relation is made by assuming that their respective heat fluxes are zero and the pressure term appearing in eq. (4) is written:

$$\frac{\partial p_i}{\partial x} = \gamma_i k_B T_i \frac{\partial n_i}{\partial x} \tag{8}$$

$$\frac{\partial p_n}{\partial x} = \gamma_n k_B T_n \frac{\partial n_n}{\partial x} \tag{9}$$

for the positive and negative ions respectively and with γ_i and γ_n taken from eq. (1).

The choice of this closure relation for the positive and negative ions imply that the system is isolated in the sense that there is no heat transfer in-between the surrounding and the system. The energy is transferred internally only in terms of work. This assumption is a simplification which allows for the hierarchy truncature of the fluid equations at the energy balance equation and represents an ideal case from a thermodynamic point of view. For the electrons, one chooses an homogeneous temperature.

The source terms S_α take into account several processes. It is convenient to analyse the results to normalize the source terms S_i, S_e and S_n to the effective ionization time τ which represents the average time between two consecutive ionizations: $S_\alpha \rightarrow S_\alpha/\tau$ for $\alpha \in$[i,e,n]. S_i is thus written as:

$$S_i = n_e - R_{ec}\, n_i\, n_n \tag{10}$$

The recombination between positive and negative ions is pondered by the recombination rate R_{ec} while the the ionization rate is proportional to n_e and the same simplifying assumption made by Gyergyek and Kovačič is chosen (see[48] and the related discussion). S_e is written as:

$$S_e = (1 - A_{tt})\, n_e + D_{et}\, n_e\, n_n \tag{11}$$

For the consistency with the positive ion source term, the first term being the ionization rate must be proportional to n_e. A_{tt} and D_{et} are the attachment and detachment rates to generate negative ions by electron attachment to a background neutral or detachment of a negative ion by electron collision.
S_n is written as:

$$S_n = A_{tt}\, n_e - D_{et}\, n_e\, n_n - R_{ec}\, n_i\, n_n \tag{12}$$

The terms M_α gives the rate of energy exchange between the positive and negative ions and other particle species because of inelastic collisions. This paper being focused on the study of the transition between the plasma and the wall and relatively low densities, one can set $M_\alpha = 0$. This implies that the species are non-interacting but not necessarily that they behave as an adiabatic flow as they are coupled through the local electric field. They can also take different temperatures depending on their formation mechanism[2]. In the following the case where the positive and negative ions have the same temperature and the case for which the negative ions have an higher temperature than the positive ions will be considered. These assumptions concerning the collisions are valid in the case of a low density plasma (around $10^{17}\mathrm{m}^{-3}$ and below for the charged particles) as considered here, and care should be taken when considering larger densities.

The following normalization variables are introduced:

$$\begin{gathered}
\lambda_d = \left(\frac{\epsilon_0 k_B T_e}{n_0 e_0^2}\right)^{\frac{1}{2}},\ c_0 = \left(\frac{k_B T_e}{m_i}\right)^{\frac{1}{2}},\ L = c_0\tau,\ \xi = \frac{\lambda_d}{L},\ N_i = \frac{n_i}{n_0},\ N_e = \frac{n_e}{n_0}, \\
N_n = \frac{n_n}{n_0},\ X = \frac{x}{L},\ \mu_i = 1,\ \mu_e = \frac{m_e}{m_i},\ \mu_n = \frac{m_n}{m_i},\ \theta_i = \frac{T_i}{T_e},\ \theta_n = \frac{T_n}{T_e}, \\
P_i = \frac{p_i}{n_0 k_B T_e},\ P_n = \frac{p_n}{n_0 k_B T_e},\ \Psi = \frac{e_0\phi}{k_B T_e},\ \eta = -\frac{d\Psi}{dX},\ V_i = \frac{u_i}{c_0},\ V_e = \frac{u_e}{c_0},\ V_n = \frac{u_n}{c_0}
\end{gathered} \tag{13}$$

---

[2] Taking the case of a low pressure negative ion source, the positive ions usually have a temperature close to the gas temperature while negative ions have significantly higher mean energies via their preferential formation mechanism

$$\mathrm{H}_2(v \geq 5) + e^- \rightarrow \mathrm{H}^{-(\mathrm{hot})} + \mathrm{H}^{(\mathrm{cold}).}$$

In eqs. (13) λ_d, c_0 and L are the Debye length, the Bohm velocity and the ionization length respectively. Provided eqs. (13), the system of equations (3-6) is then rewritten in dimensionless form for $\alpha \in$[i,e,n] as:

$$\frac{d}{dX}(N_\alpha V_\alpha) - s_\alpha = 0 \tag{14}$$

$$\mu_e N_e V_e \frac{dV_e}{dX} = N_e \frac{d\Psi}{dX} - \frac{dN_e}{dX} - \mu_e V_e s_e \tag{15}$$

For the positive and negative ions, i.e., for $\alpha \in$[i,n]:

$$\mu_\alpha N_\alpha V_\alpha \frac{dV_\alpha}{dX} \overset{i}{\underset{n}{\pm}} N_\alpha \frac{d\Psi}{dX} + \frac{dP_\alpha}{dX} + \mu_\alpha V_\alpha s_\alpha = 0 \tag{16}$$

$$\frac{1}{2} V_\alpha \frac{dP_\alpha}{dX} + \frac{3}{2} P_\alpha \frac{dV_\alpha}{dX} - \frac{1}{2} V_\alpha^2 s_\alpha = 0 \tag{17}$$

with

$$P_\alpha = N_\alpha \theta_\alpha \tag{18}$$

while the Poisson equation becomes:

$$\xi^2 \frac{d^2\Psi}{d^2X} = N_e + N_n - N_i \tag{19}$$

In the presented model, the flux of the particles reaching the wall is simply the integral of eqs. (14) for each species. As a consequence, modelling an absorbing conductive or floating wall is determined by the initial conditions for the densities, flow velocities and source terms values. For simplicity and in the rest of the paper one considers a plasma where the negative ions are mainly detached by electron impact by setting R_{ec} and A_{tt} to zero in the eqs. (10-12) for the source terms. Setting $n_0 = 1$ it follows that:

$$s_i = N_e \tag{20}$$

$$s_e = N_e + D_{et}\, N_e\, N_n \tag{21}$$

$$s_n = -D_{et}\, N_e\, N_n \tag{22}$$

The system of equations (14-19) is then mathematically converted into an explicit 1^{st} order system. The main advantage of working with the first order differential equations system is that one can perform a qualitative analysis and directly identify the singularities and initial conditions values leading to physically acceptable solutions as will be done below.

$$\frac{dN_i}{dX} = \frac{3s_i(V_i^2 - \theta_i) + N_i V_i E}{V_i(V_i^2 - 3\theta_i)} \tag{23}$$

$$\frac{dN_e}{dX} = \frac{2\mu_e V_e s_e - N_e E}{(\mu_e V_e^2 - 1)} \tag{24}$$

$$\frac{dN_n}{dX} = \frac{3s_n(\mu_n V_n^2 - \theta_n) - N_n V_n E}{V_n(\mu_n V_n^2 - 3\theta_n)} \tag{25}$$

$$\frac{dV_i}{dX} = -V_i\left(\frac{2V_i s_i + N_i E}{N_i(V_i^2 - 3\theta_i)}\right) \tag{26}$$

$$\frac{dV_e}{dX} = -\left(\frac{s_e(1+\mu_e V_e^2) - N_e V_e E}{N_e(\mu_e V_e^2 - 1)}\right) \tag{27}$$

$$\frac{dV_n}{dX} = -V_n\left(\frac{2\mu_n V_n s_n - N_n E}{N_n(\mu_n V_n^2 - 3\theta_n)}\right) \tag{28}$$

$$\frac{d\theta_i}{dX} = \frac{V_i^4 s_i + 2V_i N_i \theta_i E + 3\theta_i^2 s_i}{N_i V_i(V_i^2 - 3\theta_i)} \tag{29}$$

$$\frac{d\theta_n}{dX} = \frac{\mu_n^2 V_n^4 s_n - 2V_n N_n \theta_n E + 3\theta_n^2 s_n}{N_n V_n(\mu_n V_n^2 - 3\theta_n)} \tag{30}$$

$$\frac{d\Psi}{dX} = E \tag{31}$$

$$\frac{dE}{dX} = \frac{N_e + N_n - N_i}{\xi^2} \tag{32}$$

Furthermore, the individual terms can be analyzed separately to better understand the underlying physics as it will be done for the positive and negative ion temperatures in section III. The polytropic coefficient γ does not appear in the system (23-32). It is however straightforward to calculate γ provided its definition in eq. (1), once the solution of (23-32) is found.

B. Singularities and initial conditions

The system (23-32) represents ten equations of ten unknown functions of X: $N_i(X), N_e(X), N_n(X), V_i(X), V_e(X), V_n(X), \theta_i(X), \theta_n(X), E(X)$ and $\Psi(X)$.
Although, the system (23-32) is highly non-linear and has to be solved numerically, a qualitative analysis of the equations is possible.

Let's first start to analyse the electrons equations (24) and (27). Since the negative ions are generated in the plasma bulk, the potential is a monotonic decreasing function of space, the potential gradient E on the r.h.s is negative. As a consequence the second term is positive due to the minus sign as well as the first term of eq. (27). In eq. (27), due to the global minus sign, the numerator is thus negative. However, the fluid velocity is known to be a monotonically increasing function of space, and as a consequence this is only true when:

$$V_e - \frac{1}{\sqrt{\mu}_e} < 0 \tag{33}$$

and the system is singular beyond the electron thermal velocity defined as $V_{eth} = \mu_e^{-1/2}$. Applying the same reasoning, one observes that eq. (24) is negative as long as eq. (33) is satisfied, and thus the electron density is a monotonic decreasing function of space, as expected. This condition was also derived by Gyergyek and Kovačič[48].

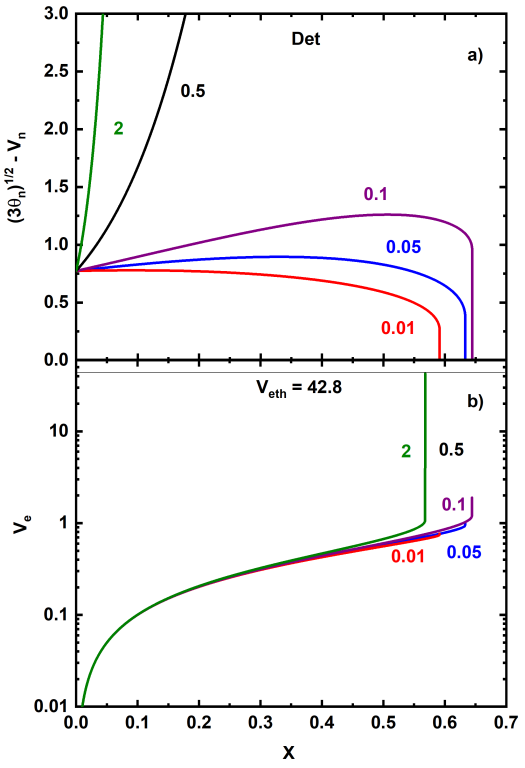

FIG. 2. a) presents the variation of the quantity $(3\theta_n)^{\frac{1}{2}}$-$V_n$ (square root of the denominator of Eq. (25)) as a function of X, b) the variation of V_e as a function of X. For both figures, the boundary conditions (36) with the source terms (38-40), $\tau = 4.7876\text{x}10^{-4}$ s and $\xi = 5\text{x}10^{-6}$ are chosen. On both figures a) and b) the curves are labelled according to the value of the detachment coefficient D_{et} for the negative ions. In b), the curves labelled 0.5 and 2 almost superimpose.

Concerning the positive ions, a difficulty arises due to the first term of the numerator being positive while the second term is negative because of the potential gradient in eq. (26). Typically, the values of the potential gradient are large and the first term of the numerator relatively small. Numerical investigations under the conditions presented in sec. III shows that the numerator is negative. Including the global minus sign in eq. (26), the positive ion velocity is a monotonic increasing function of space if:

$$V_i - \sqrt{3\theta_i} > 0 \tag{34}$$

As a consequence, if a non-zero temperature initial condition for the positive ions is chosen, the condition described in eq. (34) must be fulfilled as initial condition for V_i to obtain a physically acceptable solution. In their paper, Gyergyek and Kovačič[48] derived a similar condition: $V_i > \sqrt{\gamma_i \theta_i}$ and then found the condition given by eq. (34) in this paper by some sort of shooting method[49]. One sees here the clear advantage of working with explicit 1^{st} order system where eq. (34) could be directly derived.

Concerning the negative ions, because of the source term (see eq. 22) the first term of eq. (28) is negative, while the second is positive. There again a numerical analysis shows that for the presented conditions below in sec. III, the numerator is positive. Accounting for the global minus sign in eq. (28) and due to the fact that the negative ion flow velocity is in this case an increasing function of space it follows that:

$$\sqrt{3\theta_n} - V_n > 0 \tag{35}$$

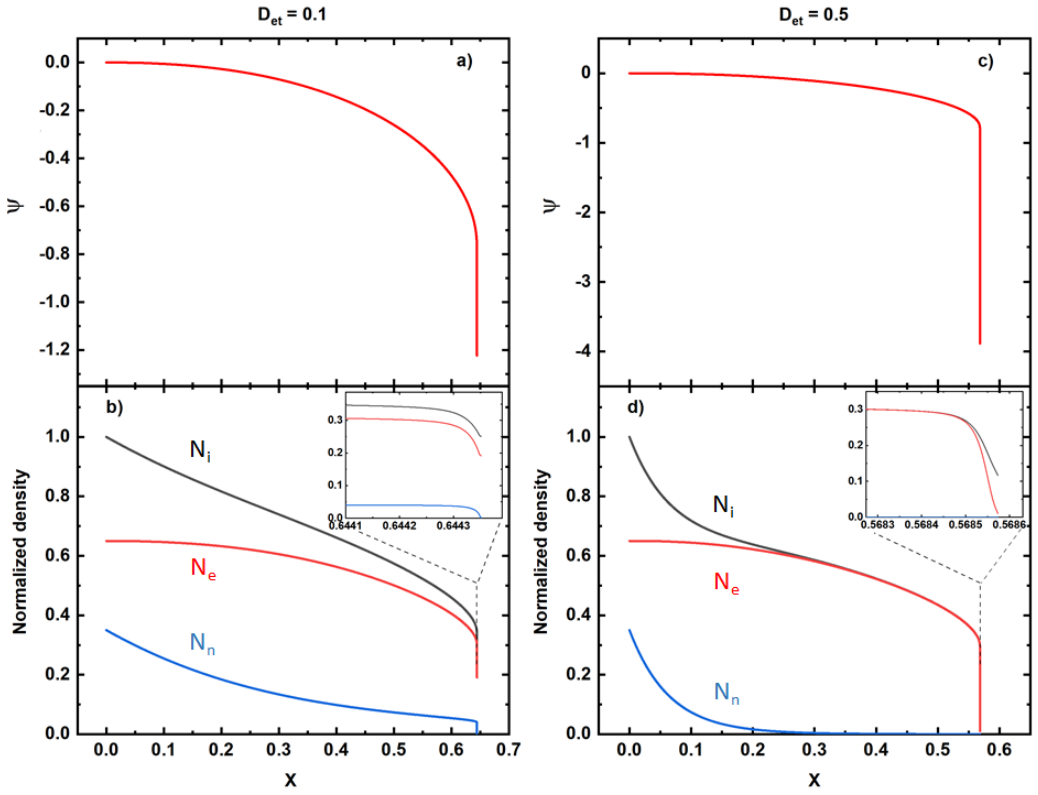

FIG. 3. a), b), c) and d) show, the potential profile and the corresponding normalized positive ion, negative ion and electron density profiles as a function of X (bottom) and Debye length (top). These results are obtained for the boundary conditions (36) with the source terms (38-40), $\tau = 4.7876\text{x}10^{-4}$ s, $\xi = 5\text{x}10^{-6}$ and $D_{et} = 0.1$ for a) and b), $D_{et} = 0.5$ for c) and d). The insets in panels b) and d) show a zoom on the sheath region.

and the system is singular beyond.

Obviously the conditions presented here are derived for a simplified model without collisions, charge exchange etc... and are also strongly dependent on the source terms.
An example showing the occurrence of the different singularities with the variation of the source terms is shown in Fig. 2 and discussed in the following section.

III. RESULTS AND DISCUSSION

A. Study of the general trends

In this sub-section, all the presented figures are obtained with the following parameters. The analysis is restricted to $\xi = 5\text{x}10^{-6}$. This value for ξ has been shown to be in the range where the asymptotic two-scale plasma-sheath approximation $\xi = \lambda_d \ / \ L \to 0$ is valid[53]. The asymptotic two-scale limit has been mathematically defined in a rigorous manner by Caruso and Cavaliere[54]. Hydrogen positive and negative ions with 1 a.m.u. are chosen. The following boundary conditions are selected:

$$\begin{gathered} N_i[0] = 1,\ N_e[0] = 0.65,\ N_n[0] = 0.35,\ V_i[0] = V_e[0] = V_n[0] = 10^{-5} \\ \theta_i[0] = 0,\ \theta_n[0] = 0.2,\ \Psi[0] = E[0] = 0 \end{gathered} \tag{36}$$

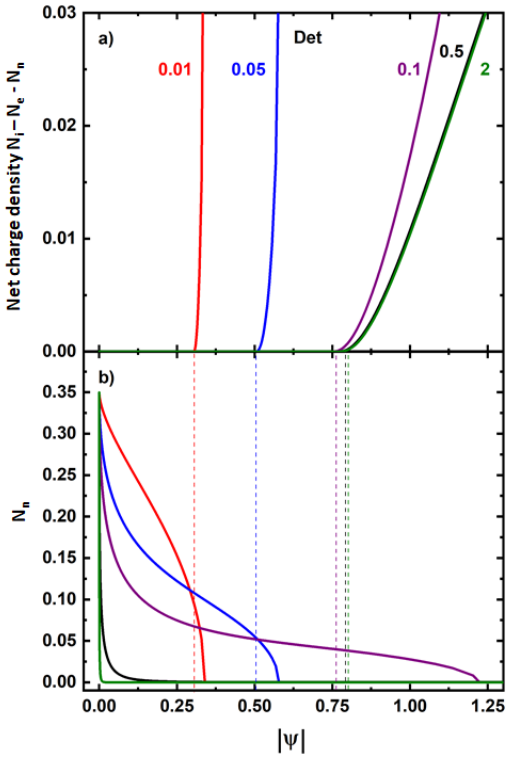

FIG. 4. a) and b) show, the net charge and negative ion densities profiles as a function of the reduced potential $|\Psi|$. These results are obtained for the boundary conditions (36) with the source terms (38-40), $\tau = 4.7876\text{x}10^{-4}$ s and $\xi = 5\text{x}10^{-6}$. The labels in a) represent the value of the detachment rate D_{et}. For each value of D_{et} and respecting the color code, the vertical dashed lines in b) are a guide to the eye to see the corresponding densities at the sheath-edge. The values n_{n-se} given in Table 1 represent the negative ion density evaluated at the sheath-edge.

With our choice of normalization, the electrons temperature is 1 everywhere. To compute the value of the source terms, one has to determine the value of τ which can be expressed, according to eqs. (13) by:

$$\tau = \xi^{-1} \left(\frac{\epsilon_0 m_i}{n_0 e_0^2} \right)^{\frac{1}{2}} \tag{37}$$

To compute τ we choose a density of $1\text{x}10^{17}\text{m}^{-3}$ and it follows that $\tau = 4.7876\text{x}10^{-4}$ s. To show our point the product $D_{et}\, N_e\, N_n$ should be small and multiplying it by τ permits to achieve the needed values. Therefore, a slightly modified version of the source terms is used:

$$s_i = N_e \tag{38}$$

$$s_e = N_e + D_{et}\, N_e\, N_n \tau \tag{39}$$

$$s_n = -D_{et}\, N_e\, N_n \tau \tag{40}$$

The only varying parameter is the detachment coefficient of the negative ions D_{et}, which will be in any case specified.

Figures 2 a) and b) present the variation of the quantity $(3\theta_n)^{\frac{1}{2}}$-$V_n$ and V_e as a function of X, respectively. The interface between the plasma and the presheath is located at $X = 0$.

On both Figures 2 a) and b) the curves are labeled according to the value the detachment coefficient D_{et} taken for the negative ions.

According to the condition derived in eq. (35), the quantity $(3\theta_n)^{\frac{1}{2}}$-$V_n$ should remain positive. Figure 2a) shows that only the curves labelled 0.01, 0.05 and 0.1 show a singularity due to this criterion. Conversely and as shown in Figure b), a singularity occurs for the curves labelled 0.5 and 2 (which almost superimpose) because the electron velocity reaches the thermal velocity defined in eq. (34), whose value for the chosen parameters is $V_{eth} = 42.8\, c_0$. Figures 2a) and b) confirm the analysis done in the previous section but also clearly show that a change of the source terms only is responsible for triggering the singularities, highlighting the fact that care should be taken with the choice of the boundary conditions.

Figures 3a), b) and c), d) present two examples of the potential profiles and the corresponding positive ion, negative ion and electron density profiles obtained for the boundary conditions specified at the beginning of this section and with $D_{et} = 0.1$ for a) and b), $D_{et} = 0.5$ for c) and d), respectively. On both panels a) and c), the potential profile starts at $X = 0$ which corresponds to the plasma side and slowly decreases in the presheath until the sheath is reached. For this reason, the potential profiles in Figures 3a) and c) reach a minimum value around -1.2 and -4.0, respectively. The influence of the detachment parameter for the negative ions can be observed in panels 3b) and d). While for both studied cases the negative ion density decreases, it is more pronounced in Figure 3d) where $D_{et} = 0.5$. For this reason in the presheath shown in Figure 3b), the quasi-neutrality is maintained by both electrons and negative ions, while one observes the positive ion density following the strong decrease of the negative ion density in Figure 3d). Furthermore, in Figure 3d) most of the negative ions are detached inside the presheath and the positive ion density then matches the electron density until the space charge separation occurs when the sheath is reached, as shown in the inset panel.

Figures 4a) and b) show the charge density and negative ion density profiles as function of $|\Psi|$ for different values of the detachment parameter. The labels in panel a) indicate the value of D_{et}. Typically, in the presheath, where the quasi-neutrality prevails the net charge density is zero, while a non-zero value is the signature of a space-charge separation, or in other words that the sheath has been reached. One observes in Figure 4a) that the space-charge separation increases faster with amount of negative ions present at the sheath-edge. This is because the negative ions, for the chosen parameters, have a temperature smaller (see Figure 6a) than the electrons and thus are more affected by the potential. The opposite effect is observed when their temperature is greater than that of electrons as will be shown below.

An increase of the detachment parameter leads to an increase of the presheath potential drop (or sheath-edge potential) and to a decrease of the negative ion density evaluated at the sheath-edge as shown in Figures 4a) and b) respectively. The values for the normalized position X_{se}, potential $|\Psi_{se}|$ and negative ion density n_{n-se} evaluated at the sheath-edge for the different D_{et} values are given in the Table 1. The trends observed in Figure 4a) and the values in Table 1 have been already shown by simpler isothermal fluid models (see for example[51,55]). Although the values for the sheath-edge potential derived in these papers cannot be directly compared to what is found here, the agreement observed for the order of magnitude of the sheath-edge potential and the fact that they obey similar trends.

D_{et}	**0.01**	**0.05**	**0.1**	**0.5**	**2**
X_{se}	0.591	0.633	0.644	0.568	0.5685
$\|\Psi_{se}\|$	0.313	0.525	0.817	0.846	0.849
n_{n-se}	0.082	0.045	0.037	0	0

TABLE I. Values of the normalized position X_{se}, potential $|\Psi_{se}|$ and negative ion density n_{n-se} evaluated at the sheath-edge for the different D_{et} values.

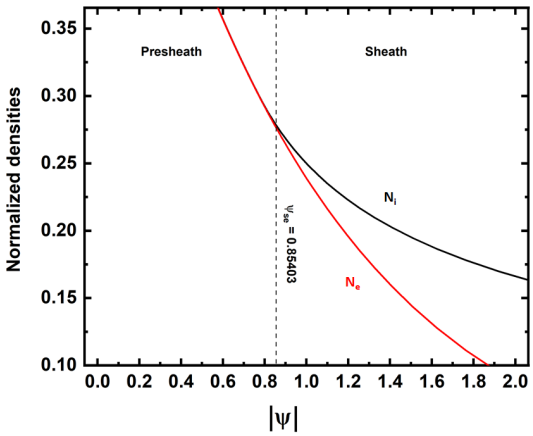

FIG. 5. Variation of the positive ion and electron density profiles a function of the normalized potential $|\Psi|$, for $D_{et} = 0.5$; the sheath-edge potential Ψ_{se} derived by Tonks and Langmuir[2] is plotted with a dash line.

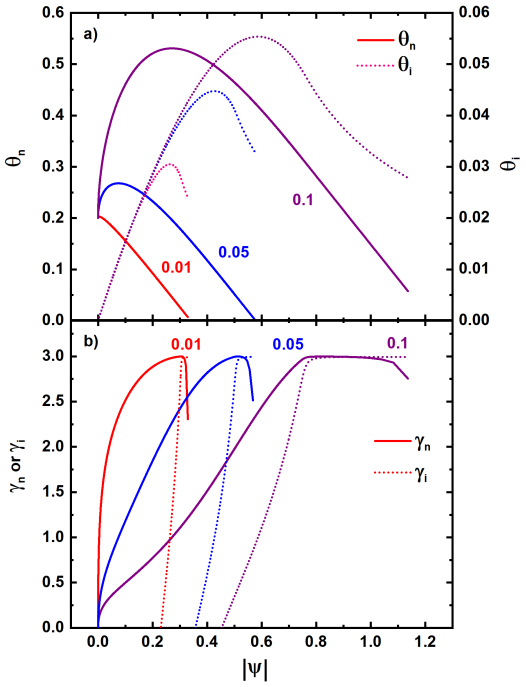

FIG. 6. a) and b) show, the variation of the reduced temperature θ_i (short dotted line) and θ_n (full line), and respectively the polytropic coefficients γ_i (short dotted line) and γ_n (full line) for D_{et} values of 0.01, 0.05 and 0.1 as a function of the reduced potential $|\Psi|$. These results are obtained for the boundary conditions (36) with the source terms (38-40), $\tau = 4.7876\text{x}10^{-4}$ s and $\xi = 5\text{x}10^{-6}$. The labels in both figures a) and b) represent the value of D_{et}.

Furthermore, one observes that for the largest values of D_{et}, namely 0.5 and 2, the negative ion density at the sheath-edge shown in Table 1 is zero and $|\Psi_{se}|$ saturates at a value around 0.85, *i.e.*, very close to the the "classical" Tonks-Langmuir value for the sheath-edge[2]. This result is highlighted in Figure 5 where it is easier to see that the sheath-edge potential for $D_{et} = 0.5$ is very close to Tonks-Langmuir value ($|\Psi_{se}| = 0.854$) plotted vertically. Note that for the case presented in Figure 5, the negative ion density has already reached zero

as shown in Figure 4b).
In the case of electropositive plasmas[49,53], it has already been shown that the Tonks-Langmuir value for the sheath-edge potential was recovered in the case of the two-scale asymptotic limit. In this work, one recovers very close values for $|\Psi_{se}|$ to 0.854 only for $D_{et} = 0.5$ and 2, both values for which the negative ion density at the sheath-edge is zero. It clearly shows, as expected, that the sheath-edge potential does not depend on the bulk n_n but only on the sheath-edge negative ion density, the two-scale asymptotic limit being fulfilled by having chosen $\xi = 5\text{x}10^{-6}$ in this study.

Figures 6a) and b) show the variation of θ_i and θ_n and γ_i and γ_n as a function of $|\Psi|$ respectively. Only the cases for $D_{et} = 0.01$, 0.05 and 0.1 are presented because most of the negative ions are detached in the presheath for larger D_{et} values as shown in Figure 4b) and Table 1.
An explanation to the trends observed for the temperatures and polytropic coefficients of both positive and negative ions, which depends on the initial conditions, will be given in the next section. One can notice that in the frame of the model assumptions, the polytropic coefficients largely vary into the presheath and the sheath. For this reason and hereafter, they will be called polytropic functions. It is not shown in Figure 6b), but the polytropic coefficient of the positive ions is highly negative for small X values (towards the neutral plasma). Negative polytropic functions are well known in astrophysics where by means of the virial theorem, one can show that a gravitating system like a star or a star cluster show an increase of temperature when loosing energy. Other examples, include self-gravitating gas sphere at thermodynamic equilibrium[56], or black hole thermodynamics[57,58]. Note that there is an obvious analogy between gravitational field and an externally applied potential gradient to a closed thermodynamic system made of charged particles[59]. However, in the presented model, for the chosen boundary conditions of $\text{N}_i[0] = 1$, $\theta_i[0] = 0$, according to the definition of γ given in eq. (1), a singularity exists at $\text{X} = \Psi = 0$. This is clearly a limitation of the model that explain the high negative values of γ_i. By choosing $\theta_i[0] > 0$ as a boundary, the singularity can be removed as will be shown in the next section.

B. Results for $\theta_i > 0$ and $\theta_n > 0$.

The results presented in this sub-section were obtained for the following initial conditions

$$\begin{gathered} N_i[0] = 1,\ N_e[0] = 0.50,\ N_n[0] = 0.50,\ V_i[0] = 0.54808758 \\ V_e[0] = V_n[0] = 3.10^{-11},\ \theta_i[0] = 0.1,\ \Psi[0] = E[0] = 0, \xi\ =\ 5.10^{-6} \end{gathered} \tag{41}$$

The same value for $\tau = 4.7876\text{x}10^{-4}$ s is chosen, with D_{et} being now fixed to 10^{-5}. The negative ion temperature at the plasma-presheath interface $\theta_n[0]$ having for values 0.10, 0.25, 0.50, 0.60 or 0.75 is the only varying parameter. The initial velocities for the electrons, positive ions and negative ions satisfy the criteria given by eqs. (33), (34) and (35) respectively.

Figure 7 shows the variation of θ_n and θ_i as a function of $|\Psi|$ for different initial conditions $\theta_n[0]$. The trends observed for θ_n resemble those shown in Figure 6a). This is however not the case for θ_i and we note that θ_i is a monotonic decreasing function of $|\Psi|$ in Figure 7. The variations of θ_i and θ_n can be easily explained by evaluating the contribution of the different individual terms of eqs. (29-30). To this aim, one defines the following terms:

$$\frac{V_i^4 s_i}{N_i V_i (V_i^2 - 3\theta_i)} \tag{42}$$

$$\frac{2 V_i N_i \theta_i E}{N_i V_i (V_i^2 - 3\theta_i)} \tag{43}$$

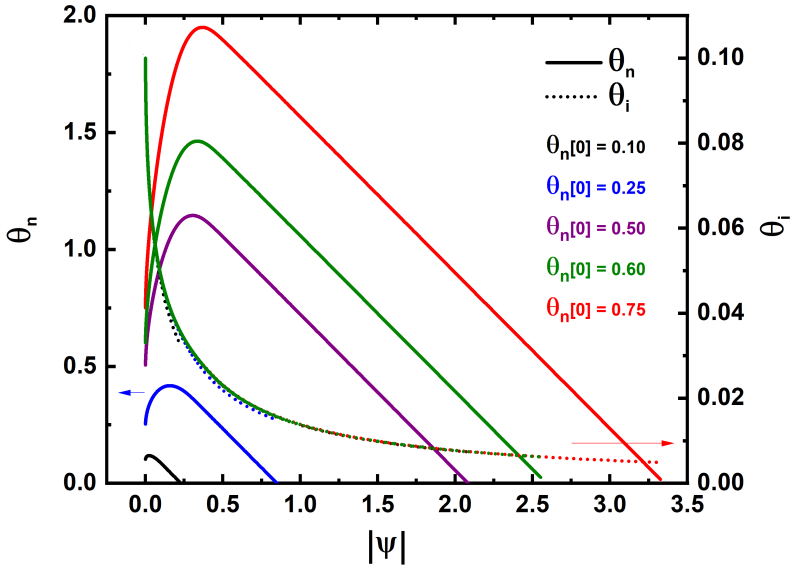

FIG. 7. Variation of θ_i and θ_n for several reduced negative ion temperatures in the plasma $\theta_n[0]$ of 0.10, 0.25, 0.50, 0.60 and 0.75 as a function of $|\Psi|$. These results are obtained for the boundary conditions (41) with the source terms (38-40), $\tau = 4.7876\text{x}10^{-4}$ s, $D_{et} = 10^{-5}$ and $\xi = 5\text{x}10^{-6}$.

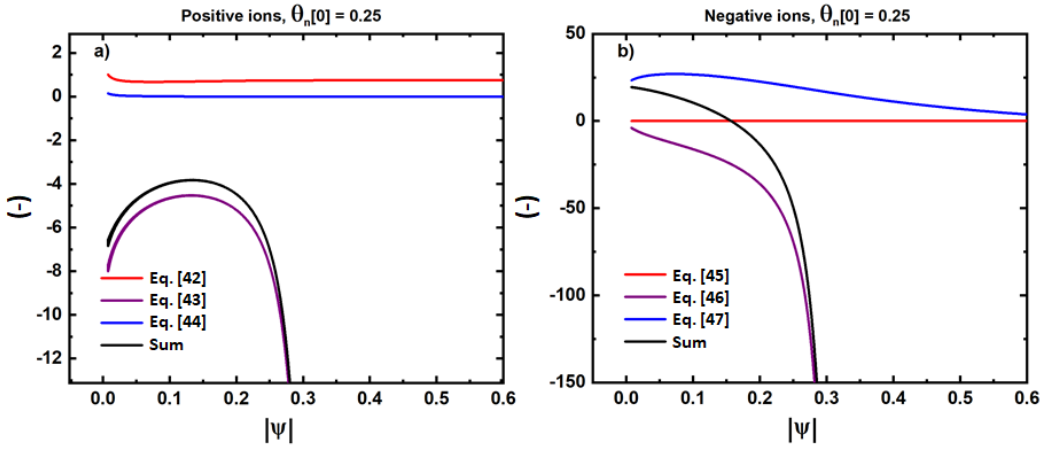

FIG. 8. Variation with the reduced potential of the different individual terms eqs. (42), (43), (44) from the positive ion temperature eq. (29) a) and the negative ion temperature, eqs. (45), (46), (47) from eq. (30) b), both for for $\theta_n[0] = 0.25$.

$$\frac{3\theta_i^2 s_i}{N_i V_i (V_i^2 - 3\theta_i)} \tag{44}$$

$$\frac{\mu_n^2 V_n^4 s_n}{N_n V_n (\mu_n V_n^2 - 3\theta_n)} \tag{45}$$

$$\frac{-2V_n N_n \theta_n E}{N_n V_n (\mu_n V_n^2 - 3\theta_n)} \tag{46}$$

$$\frac{3\theta_n^2 s_n}{N_n V_n (\mu_n V_n^2 - 3\theta_n)} \tag{47}$$

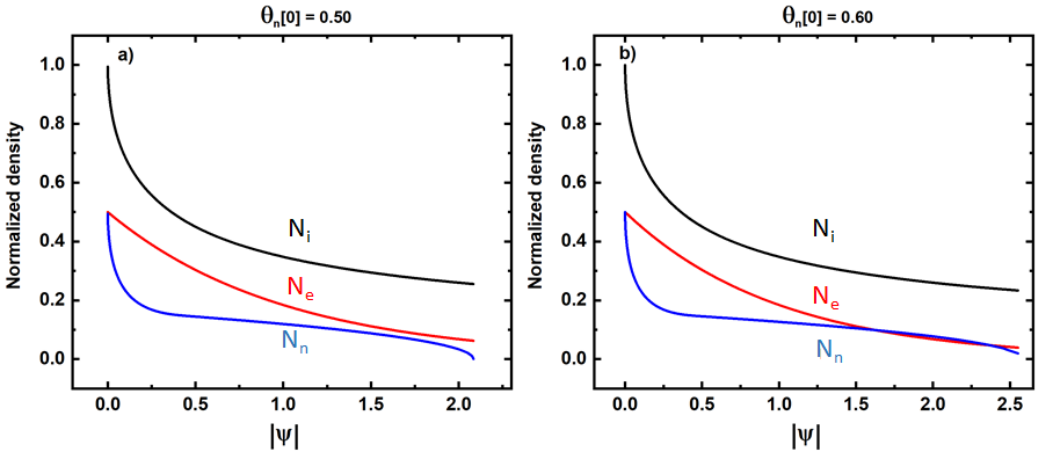

FIG. 9. Variation of the positive ion, electron and negative ions densities n_i, n_e and n_n for a) $\theta_n[0] = 0.50$ and b) 0.60 as function of $|\Psi|$. These results are obtained for the boundary conditions (41) with the source terms (38-40), $\tau = 4.7876\text{x}10^{-4}$ s, $D_{et} = 10^{-5}$ and $\xi = 5\text{x}10^{-6}$.

Eqs. (42-44) are the individual terms taken from eqs. (29) for the positive ions and eqs. (45-47) from eq. (30) for the negative ions.

Figures 8a) and b) represent the contribution of these terms for the positive ions and negative ions respectively, and as an illustrative example, this analysis is limited to the case $\theta_n[0] = 0.25$ but can be extended to the other cases shown in Figure 7a).

Let us first consider the positive ions: several mechanisms playing opposite roles can explain the trends observed in Figure 7. The first mechanism is the heating of the positive ions. Inside the presheath, at any given position X_0 with the corresponding potential Ψ_0, the velocity distribution function is smaller or equal to $\sqrt{-\Psi_0}$. The source term s_i, proportional to N_e, generates positive ions at very low temperature everywhere in the system and the potential gradient energy is converted into positive ion thermal energy. This is highlighted by eq. (42) for the positive ions in Figure 8a) being greater than 0. The second mechanism is led the potential gradient E which accelerates the positive ions towards the wall (see eq. (43) in Figure 8a)). The eq. (44) plays here no role because of the very small value chosen for $\theta_i[0]$. From Figure 8a) one clearly sees that eq. (43) dominates the dynamics of the positive ions and the sum of all the terms is everywhere negative for the chosen parameters. The potential gradient is thus the dominating term as shown in Figure 8a), explaining the continuous decrease of θ_i everywhere in the sheath and presheath.

Concerning the negative ions, the following explanations hold for both Figures 6a) and 7). First, Figure 8b) shows that eq. (45) term is negligible, which could be expected due to the very small value of both s_n and $V_n(0)$ and to the fact that $V_n(\text{X})$ stays below unity. One sees that Eq. (47) is the leading term up to $\Psi = 0.15$ and Eq. (46) beyond. Eq. (47) is positive because the chosen source term s_n is negative as well as the denominator. The potential gradient E is the leading variable of Eq. (46). As long as E is small, i.e. for $\Psi \leq 0.15$, the source term is responsible s_n for the increase of the temperature in both Figures 6a) and 7). Further downstream inside the presheath when $\Psi \geq 0.15$, E becomes the dominant parameter and is then responsible for the temperature decrease.

It is important to notice that the results concerning the temperature profiles shown in Figures 6a) and 7 clearly show that for both positive and negative ions, an isothermal, or any other constant temperature assumption fails.

Some of the consequences, on the densities, of not having an isothermal temperature for

the negative ions are shown in Figure 9a) and b) for $\theta_n[0] = 0.50$ and 0.60 respectively as a function of $|\Psi|$.
Panel a) shows the typical behaviour for low negative ion temperature. The source term s_n (see eq. 40) is proportional to both N_n and N_e. For this reason, N_n first decrease strongly, and then s_n becomes negligible as soon as N_n and N_e are small. As shown in Figure 7, an increase of $\theta_n[0]$ leads to a higher value for the maximum of θ_n. This has for consequence, that when $\theta_n > T_e$[3], $N_n[\Psi]$ decreases at a slower rate than $N_e[\Psi]$ and inversely. For this reason, by increasing $\theta_n[0]$ up to 0.50 on observes like in Figure 9a) that the negative ion density approaches the electron density. For $\theta_n[0] = 0.60$, it can be seen in Figure 9b) that N_n intercepts two times N_e: once when $\theta_n > T_e$ over a sufficient large interval of $|\Psi|$ as shown in Figure 7, and a second time inside the sheath when $\theta_n \ll T_e$ and for which $N_n[\Psi]$ decreases faster than $N_e[\Psi]$. For $\theta_n[0] > T_e$ then N_n intercepts N_e only once.
One can thus clearly see that inside the sheath the variation of the temperature influences the negative species densities to such an extent that population inversion become possible.

Figures 10a) and b) present the net charge density and γ_i (thin line) and γ_n (bold line) as function of $|\Psi|$ for different values of $\theta_n[0]$, while the vertical dashed lines in b) are a guide to the eye to see the corresponding γ_i or γ_n at the sheath-edge.
One observes in Figure 10a) that a decrease of $\theta_n[0]$ leads, as one could expect, to a faster space charge separation in the sheath, because $N_n[\psi]$ decreases faster with a lower temperature.
In Figure 10a) one can see that at the position $X = 0$, γ_i for the positive ions is equal to 3, which means that the ion flow is adiabatic. This is a consequence of having chosen $\theta_i[0] > 0$ which leads to a removal of the singularity at $X = 0$, in contrast to the results presented in Figure 6b). The profile of γ_i is in good agreement with others results[48,49,53] and can be qualitatively explained. The ion flow at the entrance of the system is adiabatic. Because the potential gradient accelerates the ions towards the wall, the ions are expanding and cooling as explained before. However, the cooling is reduced because of the heating mechanism shown in Figure 8a) due to the source term s_i and discussed before. This has for consequence that the cooling is as fast as an adiabatic cooling and γ_i decreases. Near the sheath edge, the heating mechanism becomes inefficient because N_e is small and the potential gradient is the dominant term. Thus, the positive ion flow is adiabatic again at the sheath-edge as well as inside the sheath.
Note that in Figures 7a) and 10b), the special case where $\theta_i[0] = \theta_n[0] = 0.1$ corresponds to the ions being in LTE. The trends and results being similar to the other cases is due to the electrons not being in LTE and thus the potential gradient, as discussed before, drives the ions flow towards the wall through its coupling with the electrons.

Concerning the negative ions, γ_n has a positive value close to zero at $\Psi = 0$ and then increases. The behavior of γ_n is simple to understand by rewriting eq. (1) as

$$\gamma \;=\; 1 \;+\; \frac{n}{\theta}\frac{d\theta}{dx}\left(\frac{dn}{dx}\right)^{-1} \tag{48}$$

First of all, for all the cases and everywhere in the sheath and presheath, due to s_n, one has $\frac{dn_n}{dx} < 0$. As can be shown in Figure 6a) or 7), $\frac{d\theta_n}{dx}$ is positive as long as θ_n increases and negative otherwise. When $\frac{d\theta_n}{dx}$ is positive then the second term on the r.h.s side of eq. (48) is negative, but smaller than one, the weight of this term being proportional to $\theta_n[0]$. For this reason one observes that γ_n increases at a smaller pace for increased values of $\theta_n[0]$ in

[3] T_e is isothermal with a value of 1 eV.

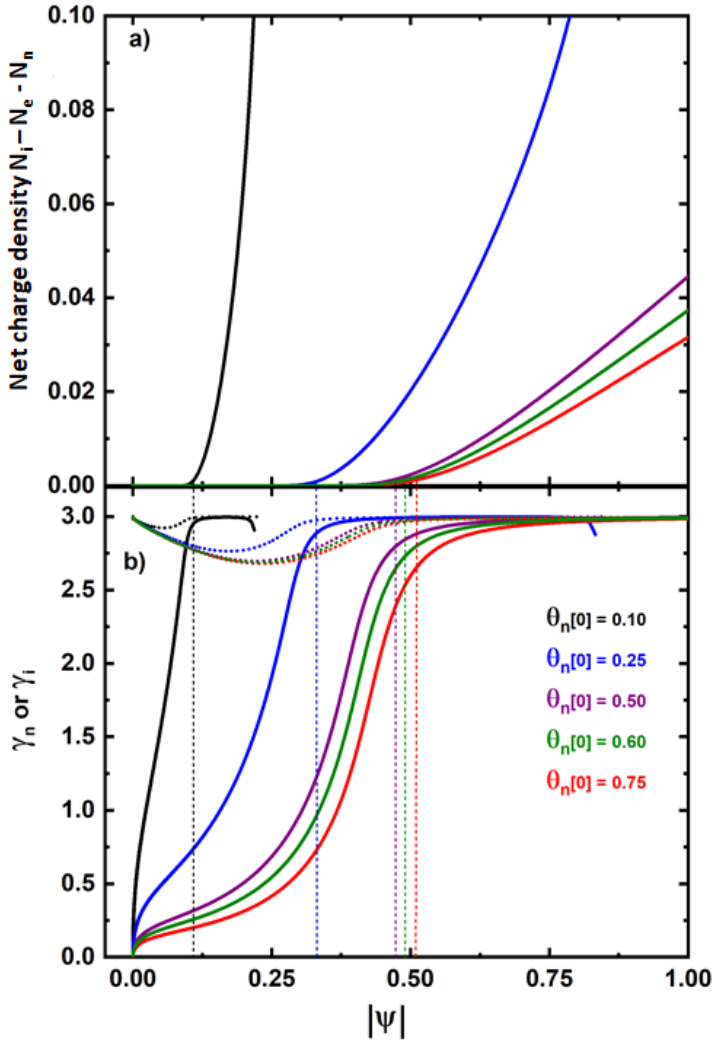

FIG. 10. Variation of the net charge density a) and γ_i (short dotted line) or γ_n (full line) b) as function of $|\Psi|$ for different values of $\theta_n[0]$. For each value of $\theta_n[0]$, the vertical dashed lines in b) are a guide to the eye to see the corresponding γ_i or γ_n at the sheath-edge. These results are obtained for the boundary conditions (41) with the source terms (38-40), $\tau = 4.7876\text{x}10^{-4}$ s, $D_{et} = 10^{-5}$ and $\xi = 5\text{x}10^{-6}$.

Figure 10. When $\dfrac{d\theta_n}{dx}$ is negative then the second term on the r.h.s of eq. (48) is positive and γ_n increases much faster. This happens as soon as θ_n starts to decrease. Thus as can be shown in Figure 10b) is the following: the negative ion flow is adiabatic at the sheath edge for the smaller values of $\theta_n[0]$ because the heating mechanism has a weaker influence. For larger values of $\theta_n[0]$ the negative ion flow tends towards adiabaticity without reaching it, because the heating of the negative ions is stronger. Nevertheless, inside the sheath, where the potential gradient strongly dominates, the negative ion flow becomes adiabatic.

The fact that one finds for both positive and negative ions that the ion flow at sheath-edge is adiabatic was expected for both having neglected the heat flux term and thermodynamics considerations. This is a very important consistency check of the presented model. As a consequence, and this is the major result of this work, it has been shown, for the first time to the authors knowledge, that the hypothesis of an isothermal negative ion temperature

with constant values for γ_n and θ_n within the sheath and presheath had to be ruled out. This is also true for the positive ions.

IV. CONCLUSION

A steady-state one-dimensional multi-fluid model has been developed for electronegative plasmas. It is an extension of a previous work[16] developed for electropositive plasmas and it accounts for the presence of negative ions, which are not assumed to be isothermal, allowing for the polytropic function to be calculated. For the positive and negative ions, the truncature of the fluid equations is made at the level of the energy-balance equation by neglecting the heat-flux term meaning that the system is isolated. The set of equations is converted into an explicit 1^{st} order system with the advantage that the singularities and the initial conditions leading to a physically acceptable result can be directly identified. Another advantage is to have the possibility of evaluating the relative importance of the different individual terms in the system of equations which allows to explain the trends of positive and negative ions temperatures θ_i and θ_n as well as γ_i and γ_n. The general trends coming out of this theory are in good agreement with the previous findings. The main new results can be summarized as follows:

- γ_n and θ_n are strongly varying functions of the space coordinate X and hence, the negative ions cannot be considered isothermal everywhere in the sheath and presheath,
- at the sheath-edge, the value of γ_n is close to 3 for low negative ion temperatures, having for consequence that the negative ion flow becomes nearly adiabatic,
- the negative ion flow is adiabatic inside the sheath.

The present results have been deduced for a detachment dominated plasma. Different behavior of the species in their way towards the wall may however be expected for an attachment dominated plasma or other conditions. While in the present study it is seen that the polytropic coefficient is a useful parameter to describe the properties of the flow of charged species, it is intriguing to note that it is done under the ideal gas law assumption (i.e. non-interacting particles). This approximation appears to yield physical results and is widely adopted in the literature with excellent results. This is a general paradox stemming from the fluid description of non-equilibrium, low ionization degree plasmas, where boundary conditions and the Poisson equation allow for the obtention of closure relations for the charged particles dynamics. Considering that initial conditions are sometimes difficult to find in order to obtain physical results, particularly for multi-dimensional models, this topic deserves further investigations in the future.

DATA AVAILABILITY STATEMENT

The data that support the findings of this study are available from the corresponding author upon reasonable request.

V. BIBLIOGRAPHY

[1]Langmuir I., Phys. Rev. 33, 954 (1929)
[2]Tonks L. and Langmuir I., Phys. Rev. 34, 876 (1929)
[3]Franklin R. N. and Snell J., J. Phys. D: Appl. Phys. 32, 2190 (1999)
[4]Lieberman M. A. and Lichtenberg A. J., Principles of Plasma Discharges and Materials Processing, New York: Wiley–Interscience (1994)
[5]Lichtenberg A. J., Lieberman M. A., Kouznetsov I. G. and Chung T. H., Plasma Sources 9 45 (2000)

[6]A. V. Vasenkov and B. D. Shizgal, Phys. Rev. E 65, 046404 (2002)
[7]Hagelaar G. J. M. and Pitchford L. C., Plasma Sources Sci. Technol. 14, 722-733 (2005)
[8]Riemann K-U, J. Phys. D: Appl. Phys. 24, 492 (1991)
[9]Tsankov T. V. and Czarnetzki U., Plasma Sources Sci. Technol. 26, 055003 (2017)
[10]Czarnetzki U., Alves, L.L., Reviews of Modern Plasma Physics, 6, 1, 31, (2022)
[11]Campanell M. D. and Umansky M. V., Phys. Rev. Lett 116, 085003 (2016)
[12]Campanell M. D. and Umansky M. V., Plasma Sources Sci. Technol. 26 (2017) 124002
[13]Schwager L. A., Phys. fluids B 5, 631 (1993)
[14]Ordonez C., Phys. Rev. E 55, 1858 (1997)
[15]Stephens K. F. and Ordonez C., Journ. App. Phys. 85, 2522 (1999)
[16]Gyergyek T. and Kovačič J., Contrib. Plasma Phys. 52, 699 (2012)
[17]Schiesko L., Wünderlich D. and Montellano I. M., J. Appl. Phys. 127, 033302 (2020)
[18]Carbone E., Graef W., Hagelaar, G., Boer D., Hopkins M.M., Stephens J.C.; Yee B.T., Pancheshnyi S., van Dijk J., Pitchford, L.., Atoms 9, 16 (2021)
[19]Atanasova M., Carbone E. A. D., Mihailova D., Benova E., Degrez G. and van der Mullen J. J. A. M., J. Phys. D: Appl. Phys. 45, 145202 (2012)
[20]Georgieva V. et al., Plasma Process Polym 14, 1600185 (2017)
[21]Tadayon Mousavi S., Carbone E. A. D., Wolf A. J., Bongers W. A. and van Dijk J., Plasma Sources Sci. Technol. 30, 075007 (2021)
[22]Mochalskyy S., Fantz U., Wünderlich D. and Minea T., Nucl. Fusion 56 (2016) 106025
[23]Revel A., Mochalskyy S., Montellano I. M., Wünderlich D., Fantz U. and Minea T., J. Appl. Phys. 122 (2017) 103302
[24]Taccogna F., Longo S., Capitelli M. and R. Schneider, Contrib. Plasma Phys. 46, 781 (2006)
[25]Schiesko L., Revel A., Minea T., Carbone E., Plasma Sources Sci. Technol. 31, 04LT01 (2022)
[26]Chapman S. and Cowling T. G., Mathematical Theory of Nonuniform Gases, Cambridge U.P. (1953)
[27]Krall N. A. and Trivelpiece A. W., Principles of Plasma Physics, McGraw-Hill New-York (1973)
[28]Braginskii S. I., Reviews of Plasma Physics, edited by M. A. Leontovich, Vol. 1, 205 (1965)
[29]Stangeby C., Phys. Fluids 27 (1984) 682
[30]Yasserian K., Aslaninejad M. and Ghoranneviss M., Phys. Plasmas 16, 023504 (2009)
[31]Hatami M. M., Shokri B. and Niknam A. R., Phys. Plasmas 15, 123501 (2008)
[32]Amemiya H., Annaratone H and Allen J. E., J. Plasma Phys. 60, 81 (1998)
[33]McAdams R., Holmes A. J. T., King D. B. and Surrey E., Plasma Sources Sci. Technol. 20, 035023 (2011)
[34]Franklin R. N., Plasma Sources Sci. Technol. 10 162–167 (2001)
[35]Gyergyek T. and Kovačič J., Phys. Plasmas 22, 093511 (2015)
[36]Allen J. E., Contrib. Plasma Phys. 48, 400 (2008)
[37]Franklin R. N., J. Plasma Phys. 78, 21 (2012)
[38]Zimmermann T. M. G., Coppins M. and Allen J. E., Phys. Plasmas 17, 022301 (2010)
[39]Kuhn S., Riemann K. U., Jelič N., Tskhakaya D. D. Sr., Tskhakaya D. Jr. and M. Stanojevič, Phys. Plasmas 13, 013503 (2006)
[40]Khoramabadi M., Ghomi H. and Shukla P. K., J. Appl. Phys. 109, 073307 (2011)
[41]Liu J, Wang F. and Sun J. , Phys. Plasmas 18, 013506 (2011)
[42]Shaw A. K., Kar S., Goswami K. S. and Saikia B. J., Phys. Plasmas 19, 102108 (2012)
[43]Chen F.F., Plasma physics and controlled fusion, second edition, Plenum press, New York and London, pp. 66-67, 94-95 (1984)
[44]Ou J. and Yang J., Phys. Plasmas 19, 113504 (2012)
[45]Fernández Palop J. I., Ballesteros J., Hernández M. A., Morales Crespo R. and Borrego del Pino S., J. Appl. Phys. 95, 4585 (2004)
[46]Fernández Palop J. I., Ballesteros J., Morales Crespo R. and Hernández M. A., J. Phys. D: Appl. Phys. 41, 235201 (2008)
[47]J.A. Bittencourt, Fundamentals of Plasma Physics, Third Edition Springer-Verlag, New York, Inc. ISBN 0-387-20975-1 (2004)
[48]Gyergyek T. and Kovačič J., Phys. Plasmas 23, 063510 (2016)
[49]Gyergyek T. and Kovačič J., Phys. Plasmas 24, 063505 (2017)
[50]Gyergyek T. and Kovačič J., Phys. Plasmas 24, 063506 (2017)
[51]Braithwaite N. St. J and Allen J. E., J. Phys. D: Appl. Phys. 21 (1988)
[52]Bredin J., Chabert P. and Aanesland A., Phys. Plasmas 221, 123502 (2014)
[53]Jelič N., Riemann K.-U., Gyergyek T., Kuhn S., Stanojević M. and Duhovnik J., Phys. Plasmas 14, 103506 (2007)
[54]Caruso A. and Cavaliere A., Nuovo Cimento 26, 1389 (1962)
[55]Franklin R. N. and Snell J., J. Phys. D: Appl. Phys. 25, 453 (1992)
[56]Lynden-Bell D., Lynden-Bell R. M., Mon. Not. R. astr. Soc. 181, 405 (1977)
[57]Beckenstein J. .D., Phys. Rev. D 9, 3292 (1974)
[58]Hawking S. W., Nature 248, 30 (1974)
[59]G. Nicolis and I. Prigogine, Proc .Natl. Acad. Sci. USA Vol.78, No.2, pp.659-663, (1981)